

Weakly bound states of two- and three-boson systems in the crossover from two to three dimensions

M. T. Yamashita,¹ F. F. Bellotti,^{2,3,4} T. Frederico,² D. V. Fedorov,³ A. S. Jensen,³ and N. T. Zinner³

¹*Instituto de Física Teórica, UNESP - Univ Estadual Paulista,
C.P. 70532-2, CEP 01156-970, São Paulo, SP, Brazil*

²*Instituto Tecnológico de Aeronáutica, 12228-900, São José dos Campos, SP, Brazil*

³*Department of Physics and Astronomy, Aarhus University, DK-8000 Aarhus C, Denmark*

⁴*Instituto de Fomento e Coordenação Industrial, 12228-901, São José dos Campos, SP, Brazil*

(Dated: February 29, 2024)

The spectrum and properties of quantum bound states is strongly dependent on the dimensionality of space. How this comes about and how one may theoretically and experimentally study the interpolation between different dimensions is a topic of great interest in different fields of physics. In this paper we study weakly bound states of non-relativistic two and three boson systems when passing continuously from a three (3D) to a two-dimensional (2D) regime within a 'squeezed dimension' model. We use periodic boundary conditions to derive a surprisingly simple form of the three-boson Schrödinger equation in momentum space that we solve numerically. Our results show a distinct dimensional crossover as three-boson states will either disappear into the continuum or merge with a 2D counterpart, and also a series of sharp transitions in the ratios of three-body and two-body energies from being purely 2D to purely 3D.

PACS numbers: 03.65.Ge, 36.10.-k, 21.45.-v

I. INTRODUCTION

Strongly interacting quantum particles are of great importance in many fields including nuclear and particle physics, condensed-matter physics, and atomic and molecular physics. However, they can be very hard to approach due to their intrinsically non-perturbative nature and often it is necessary to employ numerical simulations such as Monte Carlo [1] and/or lattice field theory techniques as done with great success in lattice QCD [2]. In the limit of few particles, strongly interacting systems can display truly remarkable features such as the Efimov effect [3] where a geometric series of three-body bound states of three bosons occur at the threshold for the binding of any two-body subsystem. This is a key insight into the often counterintuitive behavior of few-body systems that is extremely difficult to capture without analytical guidance. Moreover, it is an effect that is intimately tied to the dimensionality of space as it will not happen in two dimensions.

Cold atomic gases have proven their ability as excellent quantum simulation tools due to the tunability of interactions, geometry, and inter-particle statistical properties [4–6]. A recent frontier is the study of strongly interacting atomic Bose gases in three [7–13] and most recently in two dimensions [14, 15]. At the few-body level, three-body states linked to the Efimov effect have been observed in three dimensions [16–36] using a variety of different atomic species and two-body Feshbach resonances [37]. In spite of the tunability of the external trapping geometry of cold atomic systems, there has been little study of how the three-boson bound state problem undergoes its dramatic change from displaying the Efimov effect in three dimensions to having only two bound states in two dimensions [38]. A key question is whether it is possible

to interpolate these limits in simple theoretical terms and subsequently explore this in simulations using both more involved numerical methods and experimental setups.

Here we present a model that has the ability to interpolate geometrically between two and three spatial dimensions and thus study this important crossover for both two- and three-body bound states of identical bosons. A 'squeezed' dimension is employed with periodic boundary conditions (PBC) whose size can be varied to interpolate the two limits. It has the unique feature that it can be regularized analytically which is a great advantage for its numerical implementation allowing us to go smoothly between both limits. While PBC is not typically used in few-body calculations, it is nevertheless a standard trick when addressing larger systems [1, 39, 40] and our results may thus also serve as a benchmark. Since the seminal work of Wilson [41] and t'Hooft [42], using the dimensionality of a given model as a parameter has been a standard tool in high-energy and condensed matter physics. More recently such techniques have been applied to strongly interacting Fermi gases [43] in the context of cold atoms. Moreover, in the realm of few-body physics mixed dimensional systems are promising for extension of the Efimov scenario to new setups [44].

For many experimental setups in cold atoms, the transverse confining geometry is given by a harmonic trapping potential and a very interesting recent theoretical study [45] has considered the properties of three-boson states under strong transverse confinement. The very recent successful production of box potential traps for bosons [46, 47] means that open (hard wall) boundary conditions (OBC) are now also accessible. This still leaves the question of how to realize periodic boundary conditions in a cold atomic gas experiment. However, we would not expect large qualitative differences between OBC and

PBC and more likely only quantitative changes. This is of course also one of the reasons for employing periodic boundary conditions in most contexts throughout physics. The theoretical elegance and tractability of calculations in the three-body system is the strong incentive that we have for pursuing this geometry even if at present an experimental realization has not been found.

II. DIMER ENERGY WITH PERIODIC BOUNDARY CONDITION

In our model we will assume periodic boundary conditions along one direction (chosen to be the z -axis) which is initially a condition on the single-particle coordinates. We will now argue, however, that it may be implemented in the relative momentum which significantly simplifies its implementation. Let p_1 and p_2 be the z -components of the momenta of particles 1 and 2 with coordinates z_1 and z_2 , respectively. Then we may rewrite

$$p_1 z_1 + p_2 z_2 = Z p_{CM} + z p_z, \quad (1)$$

where $p_{CM} = (p_1 + p_2)/\sqrt{2}$ and $p_z = (p_1 - p_2)/\sqrt{2}$, while $Z = (z_1 + z_2)/\sqrt{2}$ and $z = (z_1 - z_2)/\sqrt{2}$. PBC implies that we must quantize according to $p_1 = 2\pi n_1/L$ and $p_2 = 2\pi n_2/L$, where L is the length of the periodic dimension. We thus see that p_{CM} and p_z will in turn also be quantized as a sum or a difference of a pair of integers. Furthermore, the Hamiltonian separates in CM and relative momenta. Thus we may treat p_{CM} and p_z independently.

Disregarding the center-of-mass momentum we may now concentrate on the relative part. The relative momenta along the plane are then given by $\vec{p}_\perp = (p_x, p_y)$, while

$$p_z = \frac{\sqrt{2}\pi n}{L} = \frac{n}{R}, \quad (2)$$

with $n = (n_1 - n_2) = 0, \pm 1, \pm 2, \dots$ and $L = \sqrt{2}\pi R$. The length of the squeezed dimension corresponds to a radius, R , that interpolates between the 2D limit for $R \rightarrow 0$ and the 3D limit for $R \rightarrow \infty$. In this paper we will use a contact (zero-range) interaction to study the continuous transition from 3D to 2D regimes.

Here we consider the case where we allow E_2 to vary with R under the physical condition that the magnetic field is fixed and thus we have a fixed dimer energy in 3D, E_2^{3D} . This implies that the two-body T-matrix in the limit $R \rightarrow \infty$ has to recover a pole exactly at E_2^{3D} . This means that for finite R we must solve

$$\int \frac{d^3 p}{E_2^{3D} - p^2} - \frac{1}{R} \sum_n \int \frac{d^2 p_\perp}{E_2 - p_\perp^2 - \frac{n^2}{R^2}} = 0. \quad (3)$$

As both terms in Eq. (3) are divergent, ultraviolet cut-offs that are consistent with the correct 3D limit must be introduced. It is enough to regularize the transverse momentum integral $d^2 p_\perp$ in both terms of (3) with a cutoff

Λ and then take the limit $\Lambda \rightarrow \infty$.

$$\lim_{\Lambda \rightarrow \infty} \left\{ \int_{-\infty}^{\infty} dy \ln \left[\frac{-E_2^{3D} R^2 + y^2}{-E_2^{3D} R^2 + y^2 + (\Lambda R)^2} \right] - \sum_{n=-\infty}^{\infty} \ln \left[\frac{E_2 R^2 - n^2}{E_2 R^2 - n^2 - (\Lambda R)^2} \right] \right\} = 0, \quad (4)$$

where $y \equiv R p$. Performing the analytical integration and the sum we have

$$\begin{aligned} \lim_{\Lambda \rightarrow \infty} & \left\{ \pi R \left(\sqrt{-E_2^{3D}} - \sqrt{-E_2^{3D} + \Lambda^2} \right) \right. \\ & \left. - \ln \left(\frac{\sinh \pi \sqrt{-E_2} R}{\sinh \pi \sqrt{-E_2 + \Lambda^2} R} \right) \right\} \\ & = \pi R \sqrt{-E_2^{3D}} - \ln \left(2 \sinh \pi \sqrt{-E_2} R \right) = 0. \end{aligned} \quad (5)$$

By recognizing that $\sqrt{-E_2^{3D}} \rightarrow 1/a$ in the zero-range limit (where a is the two-body scattering length), the energy of the dimer is

$$\sqrt{-E_2} = \frac{1}{\pi R} \sinh^{-1} \frac{e^{\pi R/a}}{2}, \quad (6)$$

The energy of the dimer is shown in Fig. 1. For $R \rightarrow 0$ it goes to $\sqrt{-E_2} \sim (\pi R)^{-1} \sinh^{-1} \frac{1}{2} = 0.153174 R^{-1}$, which does not depend on the scattering length. Therefore, for any 3D two-body subsystem - bound or virtual - a strong deformation of the trap towards 2D always binds the dimer with an energy given by the trap energy scale ($1/R^2$ in this case). In the unitary limit where $a \rightarrow \infty$ we find this bound state energy for any finite R . This is analogous to the famous quasi-2D harmonic trap result of Petrov and Shlyapnikov [54]. In general, the precise way in which a low-dimensional geometry is obtained will be reflected in the dimer energy formula. This is similar to Fermi gases in non-trivial confinement [55].

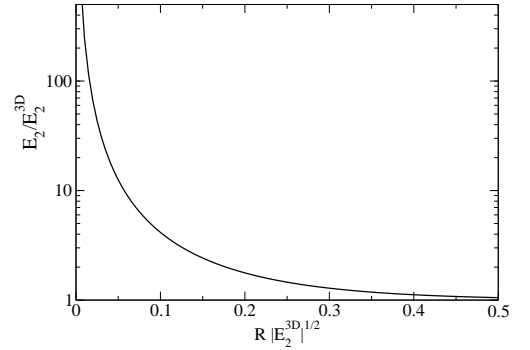


FIG. 1: Dimer energies E_2/E_2^{3D} as a function of $R\sqrt{|E_2^{3D}|}$ for periodic boundary conditions.

III. THOMAS-EFIMOV EFFECT WITH A SQUEEZED DIMENSION

The zero-range three-boson equation with a periodic dimension can be obtained as a generalization the Sko-

rniakov and Ter-Martirosian (STM) equation [48]. For completeness, let us first establish the STM equation for a regular 3D system in homogeneous space (see Ref. [49] for a discussion of the general form of the STM equations in 3D).

$$f(\vec{q}) = 2\tau_{3D} \left(E_3 - \frac{3}{4}q^2 \right) \int d^3p \frac{f(\vec{p})}{E_3 - q^2 - p^2 - \vec{q} \cdot \vec{p}}, \quad (7)$$

where E_3 is the three-body energy and $f(\vec{q})$ is the so-called spectator function which uniquely defines the three-body wave function [49]. As we only consider the equal mass case, there is only one spectator function (a detailed discussion can be found in Ref. [50]). Here τ_{3D} is the two-body T-matrix given below in Eq. (14).

We may now split the momentum variable in the directions transverse to $(p_\perp$ and q_\perp) and parallel to $(p_z$ and $q_z)$ the 'squeezed' dimension. This means that along the z -axis the momenta have to be quantized as discussed above. The integral over all momenta in the STM equation thus becomes an integral over p_\perp and a sum over the modes of the periodic dimension. Likewise, the kinetic energy (or free Green's function) is naturally split into continuous (p_\perp) and discrete contributions (p_z) . The generalized STM equation now becomes

$$f(\vec{q}_\perp, n) = 2\tau_R \left(E_3 - \frac{3}{4}(q_\perp^2 + \frac{n^2}{R^2}) \right) \times \sum_m \int d^2p_\perp \frac{f(\vec{p}_\perp, m)}{E_3 - q_\perp^2 - p_\perp^2 - \vec{q}_\perp \cdot \vec{p}_\perp - \frac{n^2}{R^2} - \frac{m^2}{R^2} - \frac{n \cdot m}{R^2}}, \quad (8)$$

where τ_R is the two-body T-matrix that we discuss momentarily (see Eqs. (11) and (12)). The parameter that interpolates between two and three dimensions is R . When R approaches zero we are effectively in 2D and in the opposite limit where $R \rightarrow \infty$ we go to the 3D case.

We now discuss the Thomas collapse [51] and Efimov effect [3]. In momentum space the matrix elements of the Dirac δ -function potential are constant. This introduces a singularity which must be resolved by proper regularization [52] which introduces a subtraction in the kernel of the zero-range three-boson integral equation, such that the properly regularized STM equations become

$$f(\vec{q}_\perp, n) = 2\tau_R \left(E_3 - \frac{3}{4}(q_\perp^2 + \frac{n^2}{R^2}) \right) \times \sum_m \int \frac{d^2p_\perp}{R} [g_{0R}(E) - g_{0R}(-\mu^2)] f(\vec{p}_\perp, m), \quad (9)$$

where

$$g_{0R}^{-1}(E) = E - q_\perp^2 - p_\perp^2 - \vec{q}_\perp \cdot \vec{p}_\perp - \frac{n^2}{R^2} - \frac{m^2}{R^2} + \frac{n \cdot m}{R^2}. \quad (10)$$

Here $f(\vec{p}_\perp, m)$ is the momentum-space three-body wave function that we need to determine. The two-body T-matrix, τ_R , is given by

$$R\tau_R^{-1}(E) = \sum_n \int \frac{d^2p_\perp}{E - p_\perp^2 - \frac{n^2}{R^2}} - \sum_n \int \frac{d^2p_\perp}{E_2 - p_\perp^2 - \frac{n^2}{R^2}}, \quad (11)$$

where $E < 0$ and we chose the bound-state pole at E_2 . Throughout most of this paper we will use units of $\hbar = \mu = M = 1$, where M is the boson mass and μ is the momentum-space subtraction point of the regularization procedure [52]. Performing the analytical integration over \vec{p}_\perp and the sum, we have

$$\tau_R(E) = -R \left[\pi \ln \left(\frac{\sinh \pi \sqrt{-E} R}{\sinh \pi \sqrt{-E_2} R} \right) \right]^{-1}. \quad (12)$$

Taking into account that the T-matrix in 2D and 3D have different units, we recover the two limits via

$$\tau_{2D}(E) = \lim_{R \rightarrow 0} R^{-1} \tau_R(E) = - \left[\pi \ln \left(\frac{\sqrt{-E}}{\sqrt{|E_2|}} \right) \right]^{-1}, \quad (13)$$

which reproduces the standard 2D amplitude [52], and for $R \rightarrow \infty$ we obtain

$$\tau_{3D}(E) = \lim_{R \rightarrow \infty} \tau_R(E) = \frac{1}{\pi^2} \left[\sqrt{E_2} - \sqrt{-E} \right]^{-1}, \quad (14)$$

valid for $E < 0$. For continuum energies, $E > 0$, the analytical extension in (13) and (14) can be performed from negative to the positive energy through the upper half of the complex energy plane. There is a subtlety in Eq. (9) since for any R the kernel is noncompact if the subtraction term is disregarded. Therefore, to take the 2D limit one has first to regularize Eq. (9) and then take the limit $R \rightarrow 0$. In addition, to get the famous 2D results of Bruch and Tjon [38], one has to also take the limit $E_2 \rightarrow 0$.

For $R \rightarrow 0$, the Efimov limit given by $E_2 \rightarrow 0$ disappears because the homogeneous Eq. (9) reduces to its usual 2D form. In this case, only states with $n = 0$ are relevant. For higher n the kinetic energy blows up and this makes terms with $n > 0$ in the kernel of the bound state equation irrelevant. The 3D Thomas collapse (infinitely negative ground state three-body energy) occurs when letting $\mu \rightarrow \infty$ in Eq. (9) after taking $R \rightarrow \infty$. For any finite R , the three-body ground state still collapses for $\mu \rightarrow \infty$ as the kernel of Eq. (9) is noncompact if the subtraction term is ignored. Here we will work in the limit where μ is finite and we take units such that $\mu = 1$ as discussed above. We note that the equivalence between the Thomas and Efimov effects that happens in 3D [53] is broken with a compact dimension.

IV. TRIMER ENERGY WITH PERIODIC BOUNDARY CONDITIONS

We now present the numerical solution of the trimer bound state equation in Eq. (9). The calculations presented are done for two different values of E_2 which are independent of R for reason of numerical convenience. In an experiment this could be achieved by using a magnetic Feshbach resonance and changing the field along with the trap size in such a manner that E_2 remains

fixed. We will address shortly what qualitative changes we expect for the case where E_2 varies with R as we have discussed in the dimer section above. Introducing explicit units for clarity, the dimensionless quantities we will use are $\epsilon_3 = E_3/E_0$, $\epsilon_2 = E_2/E_0$ and $r = R\mu/\hbar$, where $E_0 = -\frac{\hbar^2\mu^2}{M}$. In order to explore the dimensional crossover transition, Fig. 2 shows the ratios ϵ_3/ϵ_2 as a function of r for the ground, first, and second excited states. Note that the last state goes into the continuum before the 2D limit is reached.

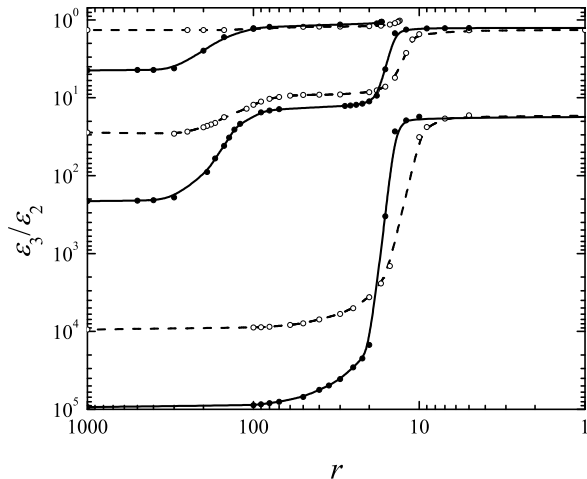


FIG. 2: ϵ_3/ϵ_2 as a function of r , for $\epsilon_2^{3D} = 10^{-7}$ (full circles) and 10^{-6} (empty circles). The solid and dashed lines are guides to the eye. As we approach the 2D limit ($r \rightarrow 0$), higher excited states disappear and only the ground and first excited states remain. Note that the values of r and ϵ_3/ϵ_2 increase from right to left and top to bottom respectively.

The points are calculated for two fixed two-body energies $\epsilon_2^{3D} = 10^{-6}$ (empty circles/dashed lines) and 10^{-7} (full circles/solid lines). In a pure 3D calculation these parameters are on the $a > 0$ side of the resonance and one finds three three-body bound states. The points at which we calculated the energies are shown explicitly, while the curves are guides to the eye. For the largest $r = 1000$, the energies were obtained from a pure 3D STM equation. The plot shows a very interesting dimensional crossover result. We have one sharp transition for the ground state and two for the first excited state, while the second excited state has two transitions before it disappears. This plot is reminiscent of the famous binding energy plot of Efimov trimers going from $a = \infty$ and into the three-body continuum [3]. The sharp jumps may also be interpreted as a sort of avoided crossing behaviour as R changes. This is very similar to what is seen in other confined systems such as short-range interacting two-body systems in a harmonic trap [56]. The latter show similar jumps as function of the ratio of the interaction and confinement energy scales and have been related to the Zeldovich rearrangement effect seen for particles

in strong magnetic fields [57, 58].

The jumps can be understood by considering the size of the trimer. It is given roughly by $\bar{r} \sim 1/\sqrt{\epsilon_3}$. For $\epsilon_2 = 10^{-7}$, from the ground state plateau at $\epsilon_3/\epsilon_2 = 93330$ for $r = 1000$ and first excited state plateau at $\epsilon_3/\epsilon_2 = 211.79$ also for $r = 1000$. From the energies in the 3D limit, we predict that for $\bar{r} = 217.29$ the ground state trimer has a size that matches the size of the squeezed dimension, r . For the first excited state the corresponding number is $\bar{r} = 10.35$. Looking at Fig. 2 we see that these numbers match quite well with the values calculated numerically. This allows us to interpret the jumps as signaling that the 2D limit is reached first for the ground state and then for the first excited state. Due to the additional avoided crossing, we get the second jump for the first excited state after which it is forced to go to the only excited state that is present in the strict 2D limit for $r \rightarrow 0$. The same analysis can be made for $\epsilon_2 = 10^{-6}$ with $\bar{r} = 10.27$ and $\bar{r} = 188.98$, respectively, for the ground and first excited state. Varying r from large to small values (left to right), the 3D \rightarrow 2D transition occurs for $r \sim 10$, where we have the disappearance of the higher (second in our case) excited states in order to reproduce the well known 2D results with two bound states proportional to $\epsilon_3/\epsilon_2 = 16.52$ and $\epsilon_3/\epsilon_2 = 1.27$ [38].

From the experimental point of view it may be difficult to keep the dimer energy, E_2 , constant. However, the transitions observed in Fig. 2 will not disappear due to a variation of ϵ_2 with r . A change in the dimer energy does not move the jumps significantly. Larger dimer energies will cause the 3D plateau to move to lower ϵ_3/ϵ_2 ratio and push the beginning of the transition to smaller r , thus making the transition region broader. In cases where there are four or more states in the spectrum, the higher states (second excited and above) will go to the continuum before one reaches the 2D limit. Whether they show two plateaus depends on whether they enter the spectrum above or below the values $\epsilon_3/\epsilon_2 = 16.52$ and $\epsilon_3/\epsilon_2 = 1.27$ in analogy to what we see in Fig. 2. In general, the jumps happen when a state is commensurate with the energy of the transverse squeezed dimension, while the associated plateaus are given by the 2D limit.

As an outlook we may consider a mass imbalanced system where the 2D limit can be much more rich with many bound states [59, 60]. This immediately implies that there could be more plateaus for these systems and that the sequence of jumps will be more involved but potentially even more interesting. We leave this issue for future studies.

The authors thank partial support from the Brazilian agencies FAPESP (2013/04093-3), CNPq and CAPES (88881.030363/2013-01), and by the Danish Council for Independent Research DFF Natural Sciences and the DFF Sapere Aude program. We thank M. Valiente and J. Levinsen for enlightening discussions

-
- [1] J. E. Drut and A. N. Nicholson, J. Phys. G: Nucl. Part. Phys. **40** 043101 (2013).
- [2] S. R. Beane *et al.*, Phys. Rev. D **85**, 054511 (2012); S. Aoki *et al.*, Prog. Theor. Exp. Phys. **2012**, 01A105 (2012).
- [3] V. Efimov, Phys. Lett. B **33**, 563 (1970) Nucl. Phys. **A362**, 45 (1981).
- [4] M. Lewenstein *et al.*, Adv. Phys. **56**, 243 (2007).
- [5] I. Bloch, J. Dalibard, and W. Zwerger, Rev. Mod. Phys. **80**, 885 (2008).
- [6] N. T. Zinner and A. S. Jensen, J. Phys. G: Nucl. Part. Phys. **40**, 053101 (2013)
- [7] S. B. Papp *et al.*, Phys. Rev. Lett. **101**, 135301 (2008).
- [8] S. E. Pollack *et al.*, Phys. Rev. Lett. **102**, 090402 (2009).
- [9] N. Navon *et al.*, Phys. Rev. Lett. **107**, 135301 (2011).
- [10] R. J. Wild *et al.*, Phys. Rev. Lett. **108**, 145305 (2012).
- [11] R. J. Fletcher *et al.*, Phys. Rev. Lett. **111**, 125303 (2013).
- [12] B. S. Rem *et al.*, Phys. Rev. Lett. **110**, 163202 (2013).
- [13] P. Makotyn *et al.*, Nature Phys. **10**, 116 (2014).
- [14] L.-I. Ha *et al.*, Phys. Rev. Lett. **110**, 145302 (2013).
- [15] V. Makhalov, K. Martiyanov, and A. Turlapov, Phys. Rev. Lett. **112**, 045301 (2014).
- [16] T. Kraemer *et al.*, Nature **440**, 315 (2006).
- [17] T. B. Ottenstein, T. Lompe, M. Kohnen, A. N. Wenz, and S. Jochim, Phys. Rev. Lett. **101**, 203202 (2008).
- [18] S. E. Pollack, D. Dries, and R. G. Hulet, Science **326**, 1683 (2009).
- [19] M. Zaccanti *et al.*, Nature Phys. **5**, 586 (2009).
- [20] N. Gross, Z. Shotan, S. Kokkelmans, and L. Khaykovich, Phys. Rev. Lett. **103**, 163202 (2009).
- [21] J. H. Huckans, J. R. Williams, E. L. Hazlett, R. W. Stites, and K. M. O'Hara, Phys. Rev. Lett. **102**, 165302 (2009).
- [22] J. R. Williams, E. L. Hazlett, J. H. Huckans, R. W. Stites, Y. Zhang, and K. M. O'Hara, Phys. Rev. Lett. **103**, 130404 (2009).
- [23] T. Lompe, T. B. Ottenstein, F. Serwane, A. N. Wenz, G. Zürn, and S. Jochim, Science **330**, 940 (2010).
- [24] N. Gross, Z. Shotan, S. Kokkelmans, and L. Khaykovich, Phys. Rev. Lett. **105**, 103203 (2010).
- [25] T. Lompe, T. B. Ottenstein, F. Serwane, K. Viering, A. N. Wenz, G. Zürn, and S. Jochim, Phys. Rev. Lett. **105**, 103201 (2010).
- [26] S. Nakajima, M. Horikoshi, T. Mukaiyama, P. Naidon, and M. Ueda, Phys. Rev. Lett. **105**, 023201 (2010).
- [27] S. Nakajima, M. Horikoshi, T. Mukaiyama, P. Naidon, and M. Ueda, Phys. Rev. Lett. **106**, 143201 (2011).
- [28] M. Berninger *et al.*, Phys. Rev. Lett. **107**, 120401 (2011).
- [29] O. Machtey, D. A. Kessler, and L. Khaykovich, Phys. Rev. Lett. **108**, 130403 (2012).
- [30] O. Machtey, Z. Shotan, N. Gross, and L. Khaykovich, Phys. Rev. Lett. **108**, 210406 (2012).
- [31] S. Knoop, J. S. Borbely, W. Vassen, S. J. J. M. F. Kokkelmans, Phys. Rev. A **86**, 062705 (2012).
- [32] P. Dyke, S. E. Pollack, and R. G. Hulet, Phys. Rev. A **88**, 023625 (2013).
- [33] S. Roy *et al.*, Phys. Rev. Lett. **111**, 053202 (2013).
- [34] S.-K. Tung *et al.*, arXiv:1402.5943 (2014).
- [35] B. Huang, L. A. Sidorenkov, R. Grimm, and J. M. Hutson, Phys. Rev. Lett. **112**, 190401 (2014).
- [36] R. Pires *et al.*, Phys. Rev. Lett. **112**, 250404 (2014).
- [37] C. Chin, R. Grimm, P. S. Julienne, and E. Tiesinga, Rev. Mod. Phys. **82**, 1225 (2010).
- [38] L. W. Bruch and J. A. Tjon, Phys. Rev. A **19**, 425 (1979).
- [39] M. G. Endres, D. B. Kaplan, J.-W. Lee, and A. N. Nicholson, Phys. Rev. A **87**, 023615 (2013).
- [40] M. Rossi, L. Salasnich, F. Ancilotto, and F. Toigo, Phys. Rev. A **89**, 041602(R) (2014)
- [41] K. G. Wilson, Rev. Mod. Phys. **47**, 773 (1975).
- [42] G. 't Hooft, Nucl. Phys. B **61**, 455 (1973).
- [43] Y. Nishida and D. T. Son, arXiv:1004.3597 (2010).
- [44] Y. Nishida and S. Tan, Few-Body Syst. **51**, 191 (2011).
- [45] J. Levinsen, P. Massignan, and M. M. Parish, Phys. Rev. X **4**, 031020 (2014).
- [46] A. L. Gaunt *et al.*, Phys. Rev. Lett. **110**, 200406 (2013).
- [47] T. F. Schmidutz *et al.*, Phys. Rev. Lett. **112**, 040403 (2014).
- [48] G. V. Skorniakov and K. A. Ter-Martirosyan, Soviet Phys. JETP **4**, 648 (1957).
- [49] M. T. Yamashita *et al.*, Phys. Rev. A **87**, 062702 (2013).
- [50] Y. Castin and F. Werner, Phys. Rev. A **83**, 063614 (2011).
- [51] L.H. Thomas, Phys. Rev. **47**, 903 (1935).
- [52] S.K. Adhikari and T. Frederico, Phys. Rev. Lett. **74**, 4572(1995).
- [53] S. K. Adhikari, A. Delfino, T. Frederico, I. D. Goldman, and L. Tomio, Phys. Rev. A **37**, 3666 (1988).
- [54] D. S. Petrov and G. V. Shlyapnikov, Phys. Rev. A **64**, 012706 (2001).
- [55] M. Valiente, N. T. Zinner, and K. Mølmer, Phys. Rev. A **86**, 043616 (2012).
- [56] T. Busch, B.-G. Englert, K. Rzążewski and M. Wilkens, Found. Phys. **28**, 549 (1998).
- [57] A. Farrell, Z. MacDonald, and B. van Zyl, J. Phys. A: Math. Theor. **45**, 045303 (2012).
- [58] N. T. Zinner, J. Phys. A: Math. Theor. **45**, 205302 (2012).
- [59] F. F. Bellotti *et al.*, J. Phys. B: At. Mol. Opt. Phys. **44**, 205302 (2011); Phys. Rev. A **85**, 025601 (2012); J. Phys. B: At. Mol. Opt. Phys. **46**, 055301 (2013).
- [60] L. Pricoupenko and P. Pedri, Phys. Rev. A **82**, 033625 (2010).